



The population dynamics of clustered consumer–resource spatial patterns: Insights from the demographics of a Turing mechanism

Zachary Hajian-Forooshani^{ab,c,1}, Iris Saraeny Rivera-Salinas^d, Ivette Perfecto^{d,1} , and John Vandermeer^a

Affiliations are included on p. 9.

Contributed by Ivette Perfecto; received April 24, 2024; accepted November 27, 2024; reviewed by David Alonso and Robert M. Pringle

In ecology, Alan Turing's proposed activation–inhibition mechanism has been abstracted as corresponding to several ecological interaction types to explain pattern formation in ecosystems. Consumer–resource interactions have strong theoretical arguments linking them to both the Turing mechanism and pattern formation, but there is little empirical support to demonstrate these claims. Here, we connect several lines of evidence to support the proposition that consumer–resource interactions can create empirically observed spatial patterns through a mechanism similar to Turing's theory. We propose the existence of a fine-scale demographic spatial pattern (DSP), in which the youngest resources are located at the periphery and oldest in the center of clusters. We find evidence of a DSP in the spatially clustered distribution of arboreal ant nests, whose large-scale spatial patterning has previously been hypothesized to be driven by ant parasitoids. Through a combination of field surveys and analysis of demographic trends, we demonstrate how the DSP structures the interactions between the ant and its parasitoid. To explore the implications of DSP for consumer–resource pattern forming systems generally, we use a spatially explicit consumer–resource model to show how relative diffusion rates of the system shape multiscale spatial patterns that structure the demographic trends of the resource population in predictable ways. This work provides both empirical support for consumer–resource spatial patterns as well as a multiscale approach to understand their spatially explicit population dynamics.

pattern formation | self-organization | consumer-resource interactions | population dynamics | agroecology

The Turing activator–inhibitor mechanism provides a qualitative understanding of self-organization of spatial patterns (1), as applied to many areas of science from chemistry (2), to cosmology (3), and in biology, from the cell to the ecosystem (4, 5). In ecology, consumer–resource interactions provide a useful analogy to Turing's conceptualization, with resources being activators, consumers inhibitors and both diffusing through space. As ecologists first began to explore spatially explicit consumer–resources models, it became clear that a variety of patterns, from traveling waves, stationary lattices, chaos, and clustered distributions, are a ubiquitous property of their spatial extension (6–11). This theoretical inevitability of spatial patterns emerging from such systems resulted in the suggestion that consumer–resource motifs may be responsible for observed large-scale spatial patterns in ecosystems (12). Although evidence for Turing-like mechanisms has been found in several empirical systems, it has rarely been attributed to consumer–resource interactions, but rather has often been abstracted to function in single-species scenarios in the form of scale-dependent feedbacks (4, 13, 14).

While there are practical difficulties in obtaining adequate spatiotemporal data to understand the dynamics of pattern formation in ecosystems, we suggest that the paucity of empirical support for consumer–resource generated spatial patterns stems in part from a lack of clear hypotheses regarding their population dynamics at multiple spatial scales. While much attention has been paid to large-scale descriptions of spatial pattern (15–17), we propose that fine-scale patterns in the constitutive elements of the larger-scale spatial pattern may be informative in understanding the mechanisms driving pattern formation. A common spatial pattern that emerges in both nature and a plethora of ecological models, including consumer–resource models, is the clustered distribution of organisms (17, 18), which are often quantified by cluster size frequency distributions (16–18). Although studying ecological spatial patterns at larger scales has been fruitful in understanding the dynamics of self-organized spatial pattern formation, we propose to couple this large-scale approach with an interrogation of the fine-scale pattern embedded within these large-scale patterns.

Significance

Alan Turing's activator–inhibitor mechanism provides a general theory to understand spatial pattern formation in ecosystems. Consumer–resource interactions, which qualitatively correspond to Turing's theory, have been hypothesized to drive some observed spatial patterns but empirical evidence has been scant. Here, we develop a framework to study consumer–resource spatial patterns by highlighting how demographic spatial patterns in clustered resources can influence trends in their population dynamics in space through time. By combining analysis of field data with modeling, we apply our approach to an arboreal ant and its parasitoid on a coffee farm in Mexico and find support for the consumer–resource interaction driving the observed spatial patterns of the ant.

Author contributions: Z.H.-F., I.S.R.-S., I.P., and J.V. designed research; Z.H.-F. and I.S.R.-S. performed research; Z.H.-F. contributed analytic tools; Z.H.-F. analyzed data; and Z.H.-F. wrote the paper with feedback from all authors.

Reviewers: D.A., Consejo Superior de Investigaciones Científicas; and R.M.P., Princeton University.

The authors declare no competing interest.

Copyright © 2025 the Author(s). Published by PNAS. This article is distributed under [Creative Commons Attribution-NonCommercial-NoDerivatives License 4.0 \(CC BY-NC-ND\)](https://creativecommons.org/licenses/by-nc-nd/4.0/).

¹To whom correspondence may be addressed. Email: zachary.hajian-forooshani@idiv.de or perfecto@umich.edu.

This article contains supporting information online at <https://www.pnas.org/lookup/suppl/doi:10.1073/pnas.2407991121/-/DCSupplemental>.

Published January 17, 2025.

With clustered spatial patterns, this means zooming-in to the scale of individual clusters to understand how processes taking place locally (i.e., at the level of the cluster) feed up to create (or at least influence) the landscape-level pattern. Furthermore, a focus on the demographic dynamics of the clusters themselves enables interrogation of the underlying mechanisms of activation and inhibition in the system at a local scale where interactions take place.

The dynamics of resource demography at the level of the cluster is presumed to be related to the mechanism of the spatial pattern formation at the larger scale. A resource population diffusing spatially (e.g., dispersing locally) suggests the existence of a demographic spatial pattern (henceforth referred to as DSP) where the oldest resources occur in the center of a cluster and the youngest on the edge. This type of demographic structure in clustered populations is likely a common phenomenon in sessile organisms that can be used to study spatially explicit population dynamics. In the context of consumer–resource interactions, the existence of DSP in the resource populations suggests several testable hypotheses: 1) While consumers randomly diffuse through space between clusters, they will first encounter the periphery of clusters where the youngest resources will be located, a basic feature of the DSP. We thus expect the highest pressure from consumers to be found on these younger resources due to their vulnerable position at the edge of clusters and the random consumer diffusion across the landscape, 2) consumers encountering younger resources will result in higher age-specific death rates for younger resources, and 3) the impact of consumers on the younger resources should depend on the relative diffusion rates of both the resource and consumer populations, as the diffusion rates will structure the prominence of the DSP in resource clusters.

To test for the hypothesized fine-scale demographic structure (DSP) and its implications on population dynamics, we leverage the well-studied consumer–resource system of a tree-nesting ant *Azteca sericeasur*, and its parasitoid, the *Phoridae* fly *Pseudacteon* spp. This empirical system's dynamics contain the two features that correspond to the classic activator and inhibitor elements of Turing's basic equations. First, the activation of resources occurs through the budding of ant colonies—queens move with a group of workers to a neighboring tree, effectively a low “diffusion” rate. The second element, inhibition, occurs via the parasitic fly-consuming ants and subsequently causing local extinction of ant nests. In the spirit of Turing's mechanism, the budding of ant nests are the activators,

which have a relatively low diffusion rate (mainly from tree to nearby tree), while the parasitoids are the inhibitors, which have a higher diffusion rate (thought to be mainly through wind dispersal). This differential diffusion, in conjunction with the antagonistic interaction between the two organisms, qualitatively corresponds to the appropriate conditions for diffusive instability and the consequent pattern formation (19, 20).

The data used to explore the hypothesized DSP and its implications come from a 45-ha plot that was surveyed annually for the presence of *Azteca* ant nests from 2004 to 2016, providing an extensive spatially explicit time series for 13 y of resource (ant nests) distribution (Fig. 1). We use this empirical dataset to demonstrate our framework for detecting the DSP in the ant population and to quantify trends in its demography through time. We couple this analysis with field surveys to confirm variation in the consumer–resource interaction strength across the demography of the ant nests. We then present a consumer–resource model and compare theoretical expectations with our empirical system to understand how the feedbacks between spatial pattern and consumer–resource interactions structure observed dynamics of the system. We find strong congruence between our data and modeling approach, suggesting that Turing's basic insight may serve as a general framework for capturing essential features of consumer–resource pattern-forming systems.

Results

Uncovering the DSP and Its Impact on Empirical Consumer–Resource Dynamics. To quantify the DSP of the *Azteca* ant nests in this system, we implement the statistical procedure outlined in Fig. 2. In short, we consider nests belonging to different age classes and quantify how the relationships between focal nests and the ages of surrounding nests within the spatial neighborhood change systematically across focal nest ages. For each focal nest age class, we performed a linear regression of the ages of neighboring nests as a function of distance to the focal nests (from the focal nests to the maximum of r) (Fig. 2*A*). The regression coefficient of the i th age class (b_i) is calculated for each of the different nest age classes (Fig. 2*B*). Given the existence of the DSP in clusters with oldest nests in the center and youngest on the edges, the qualitative prediction is that if we move away from older nests in any direction, the age of neighboring nests will decrease resulting in negative regression

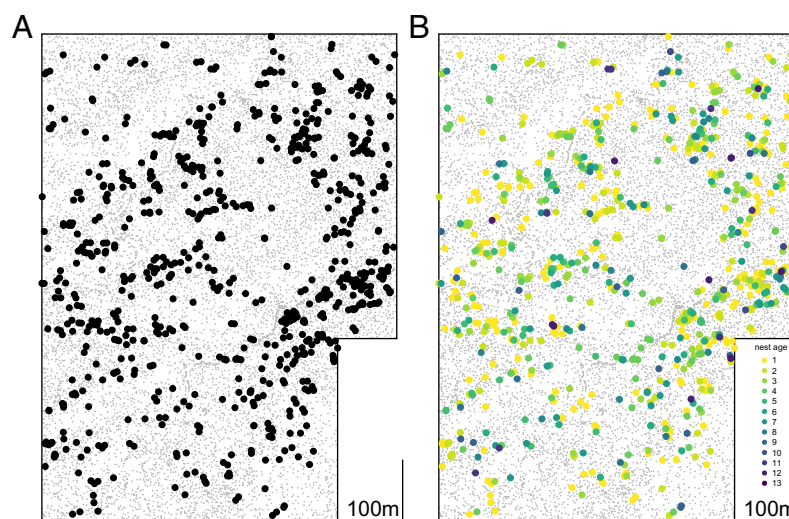


Fig. 1. Map of *A. sericeasur* ant nests on a 45-ha plot in a shaded organic coffee farm in Chiapas Mexico in 2016. (*A*) Shows the spatial distribution of the ant nests. (*B*) Shows the relative ages of nests derived from 13 y of surveys. The oldest nests in dark violet and youngest nests in yellow, and small gray symbols are shade trees that have no *Azteca* nests.

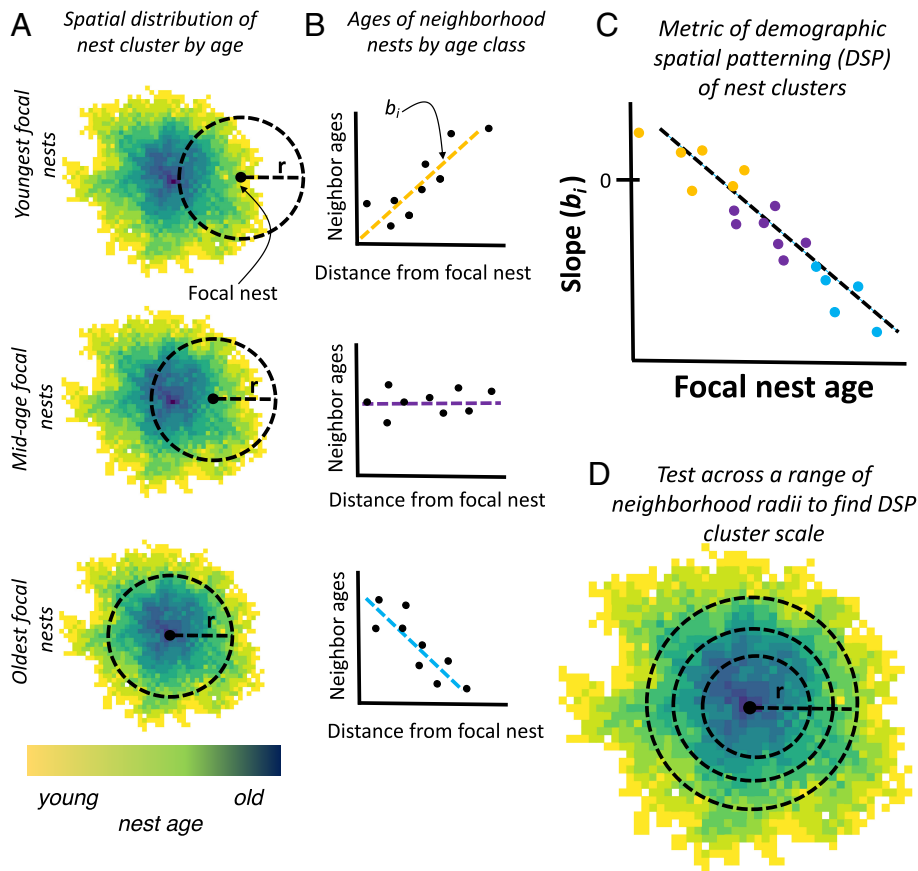


Fig. 2. Illustrating the quantification of the DSP. (A) Clustered nest age distribution in space with older nests (darker blue) in the center and younger nests (yellow) on the periphery of the cluster. (B) Relationship between nest age class and distance from focal nest for old and young nests. (C) Linear regression coefficient (b_i) as a function of the age of the focal nest. The coefficient from the regression in (C) is used to quantify the spatial demographic pattern of the nests (resources) in space. We refer to this regression as a metric of the DSP. (D) illustrates how the same test was conducted across a range of spatial scales (r) to detect the spatial scale of DSP in our system.

coefficients (b_i). However, as we move away similarly from younger nests, we expect the ages of neighboring nests to generally increase, resulting in positive regression coefficients (b_i). For intermediate age nests, we expect approximately no relationship (Fig. 2B). From this, it follows that we expect a systematic trend in these regression coefficients (b_i), transitioning from negative for old nests to positive for young nests, resulting in a negative relationship between the focal age of nests and their corresponding regression coefficients (b_i) (Fig. 2C). This negative relationship between nest age classes and their regression coefficients (b_i), which describe nest ages of their neighborhood in space, can be used as a metric of the DSP in resource clusters. Here, we take the existence of such a pattern in nest ages and regression coefficients as evidence of a DSP. Additional details regarding the procedure of quantifying the DSP can be found in *SI Appendix, S1*.

By implementing the procedure illustrated in Fig. 2 to detect the DSP across a range of spatial scales (r), we find support for a signature of the DSP in the ant nest spatial distribution. From the metric of the DSP (Fig. 2C), we see that slopes, R^2 , and P -values, support the existence of the DSP across spatial scales ranging from 13 m to 23 m on our plot (Fig. 3). By performing the test as outlined in Fig. 2 on the randomized data that shuffles the nest ages but maintains the spatial relationships between nesting sites (*SI Appendix, S1*), we can produce a null statistical expectation for our DSP metric (data in red in Fig. 3) and calculate the probability of observing our empirical metrics (the stars at the top of the plots show where the empirical measures fall outside of at least 99% of the randomized data). There are distinct scales at which we find support for DSP

when comparing empirical patterns to the randomization of nest ages (the two groups of stars in Fig. 3), suggesting that signatures of DSP in the ant nest clusters tend to be spatial scale specific. Together, these significant measures of the DSP suggest that the ant nests leave a historical trail of their diffusion, where older resources are in the center and expand out radially, forming the DSP.

Demographics of Resource Clusters Influence Consumer Dynamics.

The second component of the Turing mechanism in pattern formation is the inhibitor, which in our empirical system is represented by a *Phoridae* parasitoid fly of the *Azteca* ants. Given the DSP in the ant nest clusters as detected above, we expect to see parasitoids exerting higher pressure on the periphery of clusters (i.e., youngest *Azteca* nests) due to their random diffusion via wind dispersal which results in longer distance diffusion relative to the ants. We surveyed the parasitoid flies by disturbing *Azteca* nests of different ages and measuring 1) the time until the appearance of the first parasitoid, 2) the number of parasitoids that arrived during a 5-min interval, and 3) the duration of the parasitoid's attack. As nest age increases, the time until the first parasitoid appearance increases (Fig. 4A), the number of parasitoids decreases (Fig. 4B), and the duration of the parasitoid attack decreases (Fig. 4C). Thus, via three different measures of consumer pressure, our field surveys suggest that consumers concentrate on younger resources. Within our theoretical framework, we interpret this result as emerging from the joint combination of the DSP in the ant population and the random long-distance diffusion of parasitoids through space.

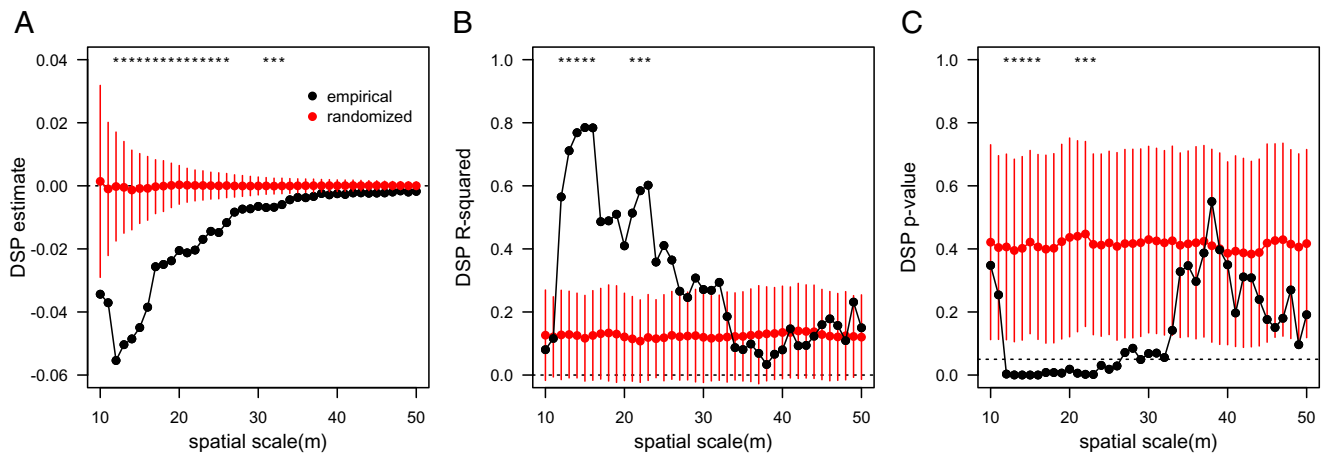


Fig. 3. DSP of arboreal ant nests as a function of spatial scale (m). The panels show the results from the regression in Fig. 2C. Black points represent the empirical data, and the red points show the results of 500 randomizations of nest ages while maintaining the actual nest spatial distribution with error bars showing the SD. The test was performed across various scales ranging from 10 to 50 m to estimate the scale of the DSP. (A) Shows the slope estimate from the DSP test, (B) the R^2 and (C) the corresponding p-value (dotted red line at 0.05). The stars at the top of each plot show where the empirical data falls outside of 99% of the randomizations.

In addition to allowing us to understand the spatial dynamics of the parasitoids with respect to the ants in our system, our field surveys allow us to explore some of their basic population dynamics. The details of consumer dynamics in the context of ecological interpretations of the Turing mechanism were explored by Alonso et al. (10), who showed theoretically that mutual interference or self-inhibition plays a critical role in the onset of pattern formation in consumer–resource systems. We searched for a signature of negative-density dependence in the relationship between increasing parasitoid numbers and the number of attacks at an ant nest. We show in *SI Appendix, S7* that our data provide some support for a signal, albeit weak, of density dependence in the per-capita attack rates of the parasitoids

Joint Impact of DSP and Consumer Dynamics on Demographic Trends of the Resource. It follows that the patterns of parasitoid attack across different ages of *Azteca* nests should influence the demographic trends in the *Azteca* population in our plot, where younger nests that experience higher pressure from parasitoids should have higher death rates. Analysis of these trends finds that the age-specific death rates of the *Azteca* ants show a clear signal of decreasing death rates as the nest age increases (Fig. 5), consistent with the expectation from the DSP in the *Azteca* population (Fig. 3) and the age-specific trends in parasitoid attack (Fig. 4). However, there is also a deviation from that trend starting at

6-y-old nests, where age-specific death rates begin to increase. The data suggest that the youngest nests on the periphery of clusters buffer older nests in the center of the cluster up until a point where the trend reverses, and there is a greater likelihood of older nests dying. This change in mortality dynamics of parasitoids on clusters at the landscape scale. A pattern previously seen from field surveys is that larger clusters of ant nests are associated with higher pressure from parasitoids (18, 21), thus making it more likely for larger clusters of ant nests to attract parasitoids. Analysis in *SI Appendix, S5* shows that older nests tend to be associated with larger clusters, supporting this explanation of two distinct regimes in death rates across the *Azteca* nest ages.

The above results taken together are consistent with the hypothesized underlying mechanisms of the system, where the diffusion process of the *Azteca* ants results in the DSP of their nests, wherein youngest nests are on the periphery and oldest in the center, which in turn structures the dynamics of the parasitoids with respect to the ages of nests encountered and attacked (Fig. 4). This differential pressure from the parasitoids then translates to the patterns of age-specific death rates of the *Azteca* nests (Fig. 5). All of these patterns are consistent with our theoretical framework, where differential diffusion of ants and parasitoids generate multiscale spatial patterns that influence their population dynamics. While there are a variety of potential mechanisms that might create patterns of

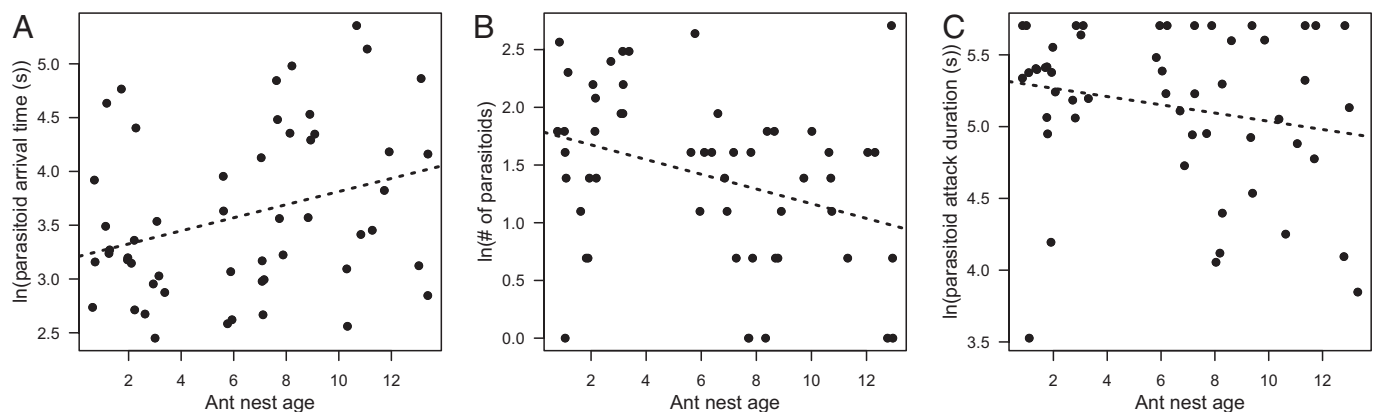


Fig. 4. Three lines of evidence that suggest parasitism is less intense for old nests (which are generally located at the center of clusters) than young nests (which are generally at the edges of clusters). (A) Shows the time until arrival, where parasitoids arrive sooner at younger nests than at older nests. (B) Shows the presence of more parasitoids at younger nests than older nests. (C) Shows a decrease in parasitoids attack as nests get older. Note that data points are randomly jittered on the x-axis to show overlapping data.

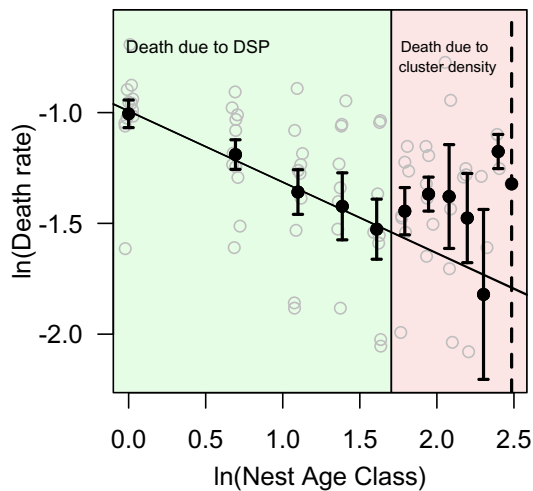


Fig. 5. Shows the average age-specific mortality for the empirical ant nest data plotted on a log-log plot. The green section shows the contribution of the DSP in the resource clusters to the age specific mortality of nests aged 1 to 5 y. The red section shows the deviation from this pattern that represents the density-dependent attack of clusters, due to older nests belonging to larger clusters. The error bars show the SE of the age-specific death rates, and the dashed line signifies a lack of variability due to a single time point in calculating the age-specific death rate for the oldest category of ant nests.

decreasing age-specific death rates, we argue that our basic framework, inspired by Turing, provides a set of minimal assumptions, capable of capturing essential features of the system. The connection between demographic trends and the diffusion parameters in our Turing-like system provides a framework to empirically interrogate the diffusion rates of the consumer–resource system and allows us to explore the utility of our framework here.

Relative Diffusion Rates and Multiscale Pattern formation.

Turing’s insight into the dynamics of pattern formation highlighted the importance of relative diffusion rates in pattern formation, and here, we show how diffusion dynamics of both consumer (inhibitors) and resource (activators) structure multiscale spatial patterns both at the landscape and at the cluster scale with the degree to which the DSP will be apparent in resource clusters. Intuitively, if consumers are dispersal limited and are diffusing relatively slowly compared to resources, then we would expect a highly pronounced DSP in the resource clusters due to the ability to spread locally uninhibited from consumer pressure. On the other hand, we expect that rapidly diffusing consumers would result in a less apparent DSP in resource clusters due to the consumers arriving at and annihilating the resources before they can create a large cluster with a prominent DSP. Thus, the presence of DSP in resource clusters will be a function of the relative diffusion rates of the consumer–resource system. This also means that the DSP may serve as a tool to approximate the underlying diffusive parameters of the consumer–resource system due to its role in structuring trends in age-specific death rates of resources (Fig. 5).

To understand the degree to which our intuition regarding the demographics of pattern-forming consumer–resource systems is informative, we use a spatially explicit consumer–resource model. We deliberately keep this model free of system-specific assumptions, as we suggest that a minimal set of assumptions regarding spatially explicit consumer–resource interactions shape the dynamics that emerge from our empirical system. We employ a stochastic individual-based framework that allows us to track demographic trends of resources and focus on the diffusion parameters of the consumers and resources, which we suggest are the driving force behind the spatial patterning and demographic

trends of the empirical ant-parasitoid system. See the methods section and *SI Appendix, S2* for details of the model and simulation approach.

Our consumer–resource model is able to recreate the previously reported self-organized clustered spatial patterning observed in other models inspired by the same system (18, 22). Consistent with our intuition, Fig. 6 shows that relatively low consumer diffusion allows for larger clusters to form in the landscape, which subsequently have a clear DSP within them. This pronounced spatial patterning of resource ages in clusters almost entirely disappears for higher values of consumer diffusion. Importantly, it is not only the cluster scale demographic patterns that change with consumer diffusion but also the landscape-scale spatial patterning of the system as well.

A measure of clustered landscape-scale spatial pattern is often quantified by fitting the frequency distribution of cluster sizes to a power law (17, 18, 22, 23). Across a range of consumer diffusion in our model, there is a systematic variation in the parameter of the power law (Fig. 7). First, as noted previously, the biggest clusters are larger with low consumer diffusion, something that is apparent on the x-axis of logged cluster size in Fig. 7. Additionally, the frequency of the smallest clusters changes across consumer diffusion rates, where we find relatively fewer small clusters at low consumer diffusion and relatively higher frequency of small clusters at high consumer diffusion. Both of these aspects of the frequency distribution of cluster sizes go on to influence the parameter of the power-law and allow us to use it as a metric for the landscape scale spatial pattern to compare to our empirical system.

Using the landscape scale spatial pattern of our empirical system, we can compare the observed frequency distribution of cluster sizes in our data with the predictions from our model. The frequency distributions of cluster sizes for the empirical (in black) and model (various colors showing replicate runs for a given parameter combination) are shown in Fig. 7 and suggest that, although there is variability between model runs, the higher consumer diffusion rates tend to better approximate the observed data. To quantify the concordance between our model and data, we first need to quantify the empirical frequency distributions across a range of spatial scales. One challenge of quantifying empirical cluster size frequency distributions is that the data are continuous in space (unlike a model bound by a lattice), which forces a decision to be made regarding the appropriate scale in which a threshold between neighboring and nonneighboring sites should be assigned. Instead of selecting an arbitrary range of spatial scales, we focused on scales in which DSP was detected in our data (Figs. 2 and 3). This range of spatial scales offers a biologically informed definition of the scale of pattern formation in the system. See *SI Appendix, S3* for details on the quantification of the empirical and simulation spatial patterns, as well as their comparison.

The range of spatial scales in which demographic structure in clusters is empirically observed is 13 m to 23 m, and the corresponding parameters of the cluster size frequency distribution range from approximately -1.6 to -1.0 (Fig. 8). Using hierarchical linear regressions, we can approximate the spatial pattern parameters from our model for the range of consumer diffusion rates. In the model, we find that when the diffusion rates of the consumers are 2.25 to 2.75 times that of the resources, the corresponding landscape-scale spatial pattern approximates our empirical system (Fig. 8).

As previously highlighted, relative diffusion rates of the consumer and resource not only impact the landscape-scale spatial patterning of the system but also the fine-scale demographic structure in the resource clusters as shown in the top row of Fig. 6. The varying strength of this DSP in the resource clusters across consumer diffusion rates suggests that the extent to which the DSP

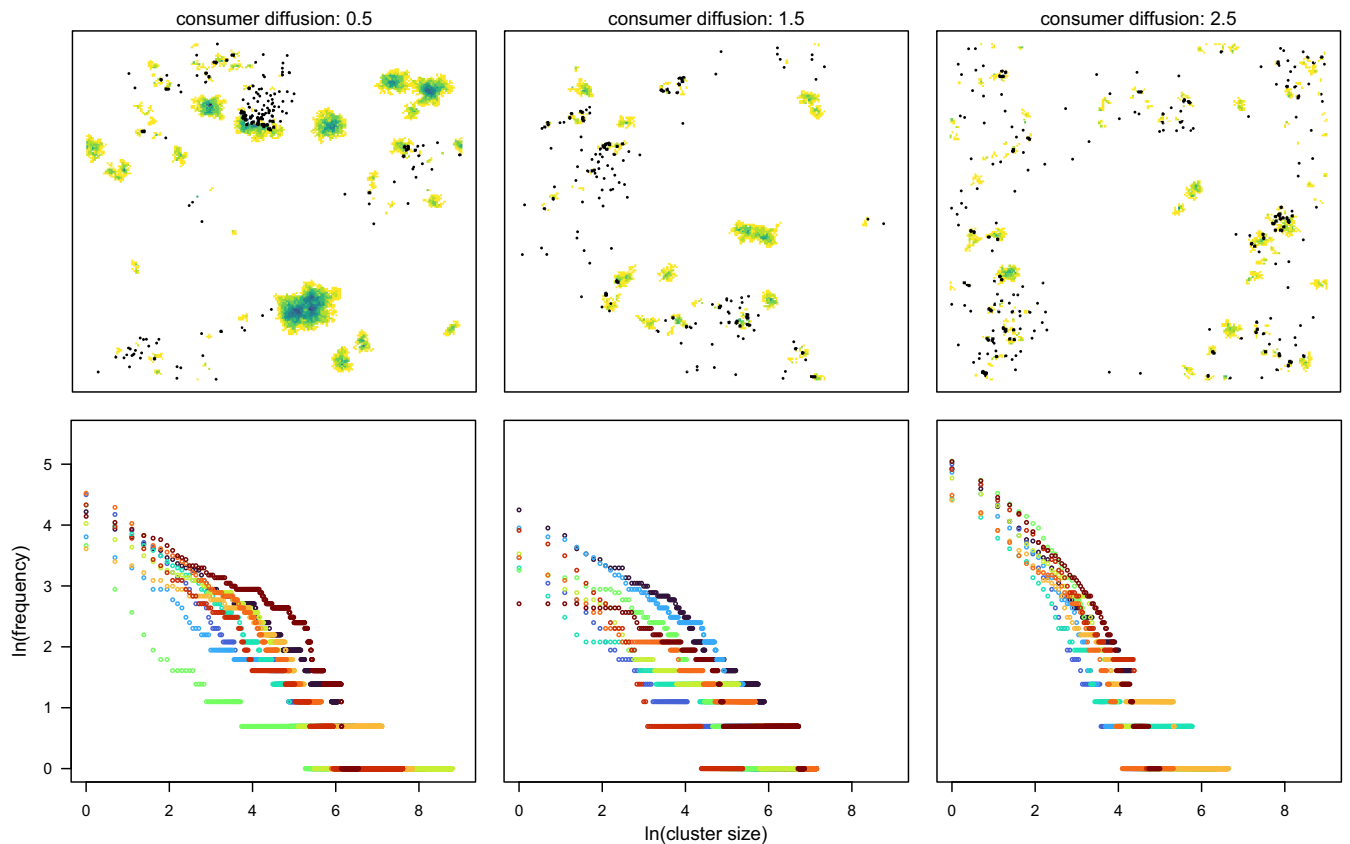


Fig. 6. Snap-shots from the individual-based model of consumer–resource interactions after 1,000 iterations. Each column corresponds to a different amount of consumer diffusion (average movement distance) while the diffusion of the resource is held constant at 1.0. The resources range in color from blue to yellow, where yellow cells represent young resources and blue old resources. The black circles on the top row represent the consumers in the model. Note that the DSP emerges most clearly in resource clusters for lower consumer diffusion, where old resources are at the center and young resources on the periphery (older = more blue and younger = more yellow). It is also clear that the consumer movement between clusters of resources will result in young resources being encountered first on the edges. The bottom row shows 10 replicates of the frequency distributions of cluster sizes that correspond to the parameters of consumer diffusion above. Visual inspection of the frequency distributions clearly shows the formation of larger clusters and few small clusters with low consumer diffusion, and this shifts to a smaller size of the largest clusters and many more small clusters under high consumer diffusion.

structures age-specific death rates of resources (as in Fig. 5) should vary as well. The age-specific death rates that emerge from the model simulations are qualitatively similar to our empirical data.

To estimate the contribution of the DSP in resource clusters to trends in age-specific death rates, we take the same approach of fitting the steeply decreasing portion of the age-specific death rate

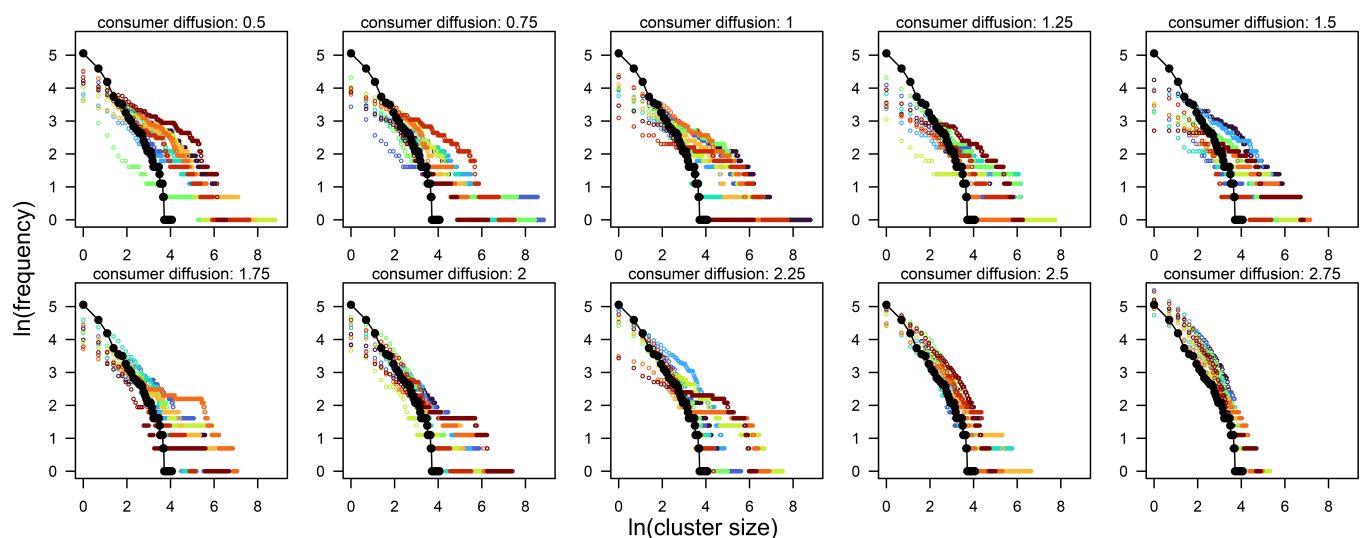


Fig. 7. Quantification of the landscape-scale spatial pattern with cluster size frequency distributions for empirical data and model. The different panels represent a range of consumer diffusion rates in the model from 0.5 to 2.75, while the resource diffusion is held at 1.0. The black points, which are the same in each panel, show the empirical cluster size frequency distribution with a neighborhood scale of 20 m (see below for scale justification). The multicolored points in each panel show the frequency distribution of the spatial patterns of a given consumer diffusion parameter for 10 replicate simulations. Note that there is variability within a parameter value due to the stochastic nature of the simulations but systematic changes in the distribution across a range of parameter values.

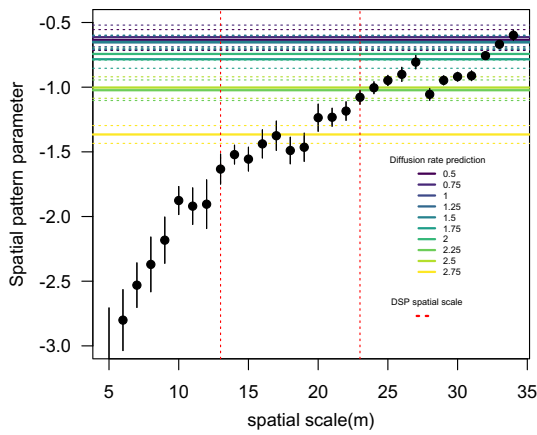


Fig. 8. Comparison of empirical and model landscape spatial pattern. Using the parameters of the power-law fit to the cluster size frequency distribution (i.e., spatial pattern parameter on the y-axis), we quantify the landscape scale spatial pattern of our observed data and the model. The black points show the empirical data with the corresponding error from the linear regression. The horizontal-colored lines show the parameter estimates from our simulation model which come from hierarchical (mixed effect) linear models that estimate the cluster size frequency distribution fit to a power-law for a given consumer diffusion parameter. The horizontal-colored solid lines show the parameter estimates and the dashed lines show the corresponding error from the statistical model. The vertical red dashed lines represent the range of spatial scales in which DSP was detected in the ages of clusters in ant nests. We used the minimum and maximum of R-squared values that fall outside 99% of the randomized simulations (Fig. 3)

curve (Fig. 9A). Comparing the parameter estimates from these linear regressions across a range of consumer diffusion values, we see that our empirical estimate is approximated by a consumer diffusion rate 2.5 to 2.75 times that of the resource diffusion (Fig. 9B). In *SI Appendix, S4*, we outline our method of approximating this decreasing portion of the age-specific death rate curve in our model data. We also explored a range of thresholds and showed that across the reasonable range of approximations for the decreasing portion of the curve; our results tell a similar story.

By confronting a spatially explicit consumer–resource model with our empirical data on the arboreal nesting ants in a coffee

farm, we are able to recover consistent approximations of the relative diffusion rates in the system from different methods at both landscape and cluster scales. Both the cluster size frequency distribution across the landscape and age-specific death rates, as structured by the DSP in resource clusters, suggest that the parasitoids (consumers; inhibitors) diffuse about 2.5 times as quickly as the ants (resources; activators).

Discussion

While there are likely multiple interacting mechanisms that generate self-organized spatial patterns in ecosystems, from scale-dependent feedbacks in mussel beds (24) to intraspecific territoriality in termites (14), there is comparatively little empirical understanding of the role of interspecific mechanisms such as consumer–resource interactions. Here, we are able to show that signatures of the pattern-generating mechanism are left behind by both the spatial distribution of resource population as well as trends in their demography. Furthermore, information regarding the differential diffusion rates of the consumer and resource, a key insight from Turing’s works on pattern formation, can be approximated through spatial patterns and demographic trends of the resource population. It seems highly plausible that qualitatively similar multiscale spatial patterns in populations should be operative elsewhere in nature and interrogatable with a similar approach to the one we present here.

The multiscale demographic lens we use in this study to understand consumer–resource systems can potentially serve as a template for further understanding the details of the many hypothesized pattern-generating mechanisms in ecology (14, 25–28). Our proposed method of studying the fine-scale patterning in clusters, the DSP, is not restricted to consumer–resource systems. Rather, we expect such demographic patterns to be present to some degree in locally diffusing clustered populations generally. In pattern-forming systems where the dynamics of clusters are the focus of investigation (e.g., refs. 23, 28, and 29), the dynamics of DSP may inform the underlying parameters driving pattern formation. Although the expected relationship between demographic trends and the parameters of pattern formation will be mechanism-specific, DSP offers

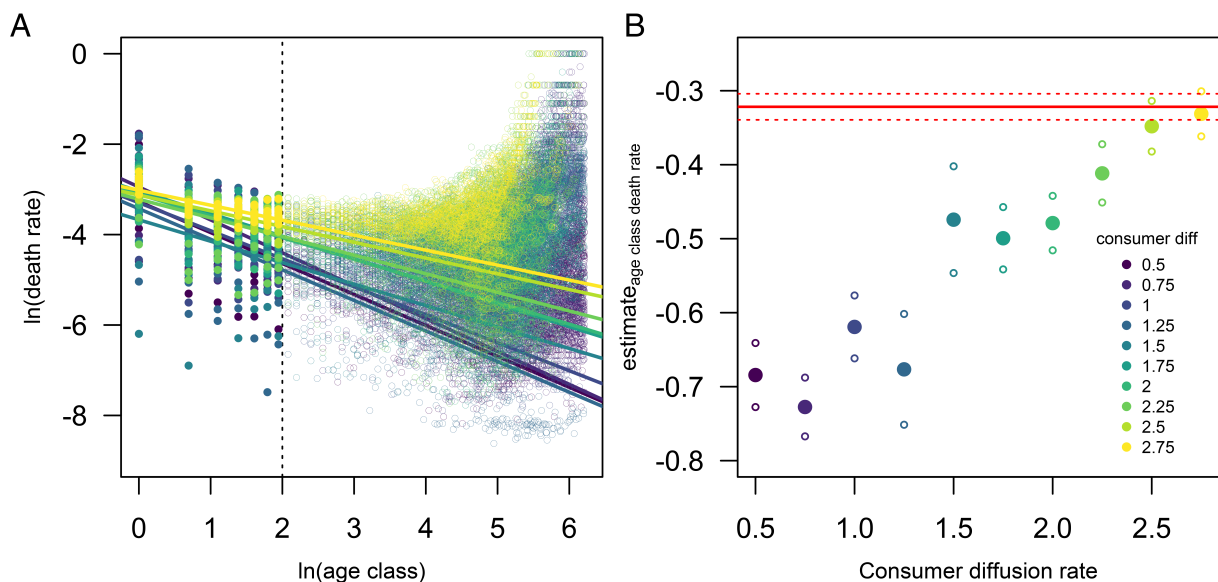


Fig. 9. Age-specific death rates of resources as structured by the DSP of resource clusters. (A) Shows a plot of the age-specific death rates for model simulations across a range of consumer diffusion rates. The colors of points correspond to consumer diffusion which is noted in the legend on B and the dashed line shows the threshold for which we ascribe the trend in death rates to be due to the DSP in resource clusters. Note that a similar plot for the empirical data is seen in Fig. 5. (B) Shows the parameter estimates from panel (A) across the consumer diffusion rates. The horizontal red line shows empirical parameter estimate (the slope of the line on Fig. 5) and the associated error with the dashed lines.

a novel unit of measurement that may help make connections between theoretical approaches and empirical systems. Quantifying various ecologically relevant quantities that emerge from spatial pattern-forming models to compare to empirical data is particularly important, given that multiple mechanisms can generate qualitatively similar large-scale spatial patterns (see ref. 29). Attempts to more robustly link mechanisms to patterns will likely require moving beyond single-scale model-data comparison in addition to experimental approaches.

Although we have shown that demographic trends, which we measure with a DSP, as well as metrics of landscape-scale spatial pattern, both approximate similar values of relative diffusion rates of the ant-parasitoid system, the approximations emerge from measurements interpreted through our conceptual and modeling frameworks. An important next step would be to directly verify the approximations of the underlying parameters of ant and parasitoid diffusion in the natural system. Apart from detailed work on the natural history of the system across large spatiotemporal scales, it may be possible to directly approximate diffusion rates with a spatially explicit population genetic study of the ants and parasitoids. Bradburd and Ralph (30), for example, note that a spatial pedigree might be used to quantify ecological parameters such as dispersal. Similar approaches to spatially explicit population genetics studies offer potentially promising ways to more directly quantify diffusion rates of pattern-forming systems when not easily obtainable by other methods (31, 32). Although population genetics approaches in service of furthering our understanding of self-organized pattern formation are not widely employed (although there are exceptions, e.g., refs. 33 and 34), we suggest that useful insights into the underlying mechanisms may emerge with such approaches.

While we suggest that Turing's theory of pattern formation serves as a useful organizing metaphor to understand the system in this study, it is worth noting that the system does not meet the formal criteria of the Turing mechanism or diffusive instability in the strict sense of these terms. Our modeling framework, which is both individual-based and stochastic, prevents us from conducting traditional analysis of diffusive instability and does not seem to produce the classical fixed spots and stripes often associated with Turing's partial differential equation model (10, 15, 28, 35). Although not "strictly Turing," our approach highlights how Turing's basic insights regarding the importance of activation/inhibition and the relative diffusion rates in the system remain an essential component in self-organized spatial patterns even outside of the particular mathematical formulations often considered.

Here, we have highlighted some of the basic expectations regarding the population dynamics of pattern-forming consumer-resources systems and attempted to show how they can be interrogated empirically with a multiscale framework. While our study emphasizes the consumer-resource mechanism as a driver of pattern formation, it is important to acknowledge that multiple mechanisms likely interact and contribute to realized spatial patterns in our system. For example, prior analysis of the spatial dynamics of *Azteca* suggests that exogenous factors (i.e., tree density) likely contribute modestly to pattern formation (36). Furthermore, a number of endogenous factors have been proposed to drive the observed patterns of density dependence in *Azteca's* spatial dynamics. Several of these mechanisms are thought to operate through a mutualistic association between *Azteca* and the scale insect, *Coccus viridis*, where *Azteca* increases the population of scale insects locally until natural enemies of the scale arrive to decimate the scale population, which results in the subsequent mortality of *Azteca* nests due to loss of a vital resource (37). A predatory Coccinellidae beetle, *Azya orbiger*, and an entomopathogenic

fungus, *Lecanicillium lecanii*, have both been proposed as influencing the spatial pattern formation of *Azteca* through their interactions with the scale insects (37–39). While we highlight the role of the *Phoridae-Azteca* consumer-resource interaction as the primary mechanism of pattern formation in our system, this interaction only occurs within the context of a complex ecological network, which undoubtedly contributes to the dynamics of pattern formation (37, 40). Understanding the relative contributions of multiple interacting mechanisms of pattern formation, both endogenous and exogenous, remains an important and open challenge for our system as well as others like it (14).

It is likely that most ecological processes, including those that drive pattern formation, act at distinct and interacting spatial scales (41–45). Here, we have presented a multiscale approach to understanding pattern formation in consumer-resource systems empirically and attempted to illustrate how the original spirit of Turing's insights into activator-inhibitor systems seen through a demographic lens can be applied to ecological systems. Through multiple lines of evidence, we show how the dynamics of fine-scale demographic spatial structure in clustered resource populations can lend insights into the processes that generate large-scale spatial patterns. We propose the existence of a DSP in resource populations and illustrate how it can structure the spatiotemporal population dynamics of consumer-resource systems. We also demonstrated how to approximate information on the diffusive dynamics of the consumer-resource system through a multiscale analysis of fine-scale and large-scale spatial patterns and demographic dynamics. By focusing on basic assumptions that stem from the spatially explicit population dynamics of consumer-resource systems, we suggest progress can be made toward a general understanding of consumer-resource pattern-forming systems.

Materials and Methods

Phoridae Parasitoid Dynamics Across *Azteca* Nest Demography. *Azteca* ant nests were haphazardly selected from the database to measure *Phoridae* dynamics across a range of *Azteca* nest ages on the 45-ha plot on a coffee agroecosystem in southern Mexico. Once at the site of an *Azteca* nest, we slowly approached the tree containing the ant colony and attempted to identify where the majority of ant activity was prior to disturbing the nest. We subsequently killed 10 ants in an area of high activity by pressing them into the trunk of the tree. During the killing process, a stick or leaf was used to kill the ants and left at the site as to not carry *Azteca* pheromones between sites. Once the first ant was killed, we started a stopwatch to time how long it takes for the first *Phoridae* parasitoid-fly to arrive to the local site of the disturbance. Once a *Phoridae* was spotted, we turned off one stopwatch and triggered another one to measure the duration of the attack. While the *Phoridae* were present at a site, we monitored the number that arrived, the number of successful attacks, and the duration of the total attack for up to 5 min. If there were no successful attacks for 1 min, then we considered the attack from parasitoids to be finished.

To analyze the trends in the *Phoridae* dynamics across the ages of *Azteca* nests, we used Bayesian multilevel models implemented in the brms R package (46). The structure for our three separate models which modeled 1) the number of *Phoridae*, 2) the time to first arrival, and 3) the duration of the attack, were kept consistent. All response variables were log-transformed, and models included both *Azteca* nest age as well as the circumference of the tree in which the nest was occupying as fixed effects. The identity of the hectare that the nesting tree occupied was included as a random effect (on the y-intercept) in the models. Additional details on model structure and output can be found in *SI Appendix, S6*.

Long-Term Data Collection of Nest Locations (2004 to 2016). Each tree on a 45-ha plot in a coffee agroecosystem in southern Mexico has been surveyed to look for the presence of *Azteca* nests since 2004. Data from this survey are used here from 2004 through 2016, to pick sites for fieldwork and also to look for trends in *Azteca* nest demography.

Analysis of Long-Term Data. To calculate the age-specific death rates of the nests, we calculated the change in number of nests from 1 y to another divided by the number of nests in that age class. Doing this each year, we have the age-specific death rates on an annual basis. It is important to note that while we call these death rates, they are, in essence, “disappearance” rates or extinction rates in Levin’s sense of the term. Since the survey consists of checking to see whether ants are occupying a given tree, we cannot say with certainty whether that nest died or moved from one tree to another. Furthermore, we cannot definitively attribute nest disappearance to the parasitoids in the system. Given the lack of information on the natural history of this species and the spatial-temporal scales of the data we use here, it is unclear how one might make the distinction between the two processes and their ultimate cause.

Model Description. The resource (which corresponds to ant nests in the empirical system) dynamics occur on a 100x100 lattice with periodic boundary conditions where each space represents a site which can contain a single resource population. The resources are bound to the cells inside of the lattice, and when a resource population has been established, we here refer to it as a resource-site. For each iteration, every established resource-site increases its resource-energy by 1 unit and increases its resource-age by 1 unit. Resource-sites can only diffuse locally to unoccupied sites in their Moore-neighborhood (the 8 cells surrounding a focal cell), effectively giving them a diffusion rate of 1 unit of space. This scale of local diffusion of resources is held constant for all of the simulations and has a fixed probability of, ρ , for each iteration of the model. If a resource-site successfully establishes another resource-site in its local spatial neighborhood (via some fixed probability), then the “parent” resource-site divides its energy by κ . The new resource-site starts with 1 unit of resource-energy.

The consumers (which correspond to the parasitoid *Phoridae* flies in our empirical system) are represented in the model as a distinct agent with energy values gained from the consumption of resources and lost during their lifetime. Consumers are randomly initialized on a given fraction, β , of resource-sites. The diffusion process of the consumers is distinct from that of the resources in the model. Instead of being bound by the cells in the lattice, the consumer diffusion is implemented continuously across the landscape with random walks. The facing angle of the consumers is randomly drawn from a uniform distribution, and then, a step length is drawn from a Gaussian distribution with mean, λ , and a SD of 1.

When a consumer encounters a resource-site, it stops its diffusion through space and begins reducing the resource-energy of the resource linearly by

α and converts it linearly into consumer-energy (i.e., by α). If the resource-energy reaches zero, the resource-site goes extinct in that cell and the consumer continues to diffuse across the landscape with a random walk. When a given consumer’s energy surpasses the threshold, ϕ , it then produces a new consumer resulting in the parent consumer’s consumer-energy being divided by, Ω . The newly created consumer inherits the consumer-energy which was lost from the parent consumer. Finally, the consumers have a baseline consumer-energy cost, ϵ , that linearly decreases consumer-energy as they diffuse through space. If consumer-energy reaches or surpasses zero then the consumer dies.

Additional information on the model, including pseudocode and parameters for the simulations, can be found in *SI Appendix, S2*. The model was implemented in NetLogo 6.0 (47) and can be found as a “.nlogo” file in supporting material.

Data, Materials, and Software Availability. All data and code are publicly archived and open here: https://figshare.com/projects/The_population_dynamics_of_clustered_consumer-resource_spatial_patterns_insights_from_the_demographics_of_a_Turing_mechanism/224382 (48, 49).

ACKNOWLEDGMENTS. We would like to thank Gustavo López Bautista and Braulio E. Chilel for managing data collection in Mexico; the Peter’s family and Walter Peters for allowing us to conduct research on their coffee farm and; Chatura Vaidya, Kristel Sanchez, Tamara Milton, Paul Glaum, Douglas Jackson, David Allen, Jonno Morris, and Kevin Li for feedback on ideas and earlier versions of the manuscript. Ferdinand LaMothe, Earl Hines, and Sidney Bechet provided inspiration. Portions of the present manuscript were also part of the PhD dissertation of Z.H.-F. Z.H.-F. was supported by the Agriculture and Food Research Initiative (AFRI) Predoctoral Fellowship [Grant No. 13374090/Project Accession No. 2022-6701136581] from the United States Department of Agriculture (USDA) National Institute of Food and Agriculture. Additional funding support came from USDA Grants NIFA/USDA 20172017-67019-26292326292 and NIFA/USDA 2018-67030-28239.

Author affiliations: ^aDepartment of Ecology and Evolutionary Biology, University of Michigan, Ann Arbor, MI 48104; ^bGerman Centre for Integrative Biodiversity Research (iDiv), Halle-Jena-Leipzig, Leipzig, Germany 04103; ^cInstitute of Computer Science, Martin Luther University Halle-Wittenberg, Halle (Saale), Germany 06099; and ^dSchool for Environment and Sustainability, University of Michigan, Ann Arbor, MI 48109

1. A. M. Turing, The chemical basis of morphogenesis. *Philos. Trans. R. Soc. Lond. B* **237**, 37–72 (1952).
2. J. Horváth, I. Szalai, P. De Kepper, An experimental design method leading to chemical Turing patterns. *Science* **324**, 772–775 (2009).
3. T. Nozakura, S. Ikeuchi, Formation of dissipative structures in galaxies. *Astrophys. J.* **279**, 40–52 (1984).
4. M. Rietkerk, J. Van de Koppel, Regular pattern formation in real ecosystems. *Trends Ecol. Evol.* **23**, 169–175 (2008).
5. S. Kondo, T. Miura, Reaction–diffusion model as a framework for understanding biological pattern formation. *Science* **329**, 1616–1620 (2010).
6. H. N. Comins, M. P. Hassell, R. M. May, The spatial dynamics of host-parasitoid systems. *J. Anim. Ecol.* **61**, 735–748 (1992).
7. E. McCauley, W. G. Wilson, A. M. de Roos, Dynamics of age-structured and spatially structured predator–prey interactions: Individual-based models and population-level formulations. *Am. Nat.* **142**, 412–442 (1993).
8. R. V. Sole, J. Valls, J. Bascompte, Spiral waves, chaos and multiple attractors in lattice models of interacting populations. *Phys. Lett. A* **166**, 123–128 (1992).
9. J. Bascompte, R. V. Solé, Rethinking complexity: Modelling spatiotemporal dynamics in ecology. *Trends Ecol. Evol.* **10**, 361–366 (1995).
10. D. Alonso, F. Bartumeus, J. Catalan, Mutual interference between predators can give rise to Turing spatial patterns. *Ecology* **83**, 28–34 (2002).
11. M. Baumann, T. Gross, U. Feudel, Instabilities in spatially extended predator–prey systems: Spatiotemporal patterns in the neighborhood of Turing–Hopf bifurcations. *J. Theor. Biol.* **245**, 220–229 (2007).
12. J. L. Maron, S. Harrison, Spatial pattern formation in an insect host-parasitoid system. *Science* **278**, 1619–1621 (1997).
13. J. Schoelynck *et al.*, Self-organised patchiness and scale-dependent bio-geomorphic feedbacks in aquatic river vegetation. *Ecography* **35**, 760–768 (2012).
14. R. M. Pringle, C. E. Tarnita, Spatial self-organization of ecosystems: Integrating multiple mechanisms of regular-pattern formation. *Annu. Rev. Entomol.* **62**, 359–377 (2017).
15. C. A. Klausmeier, Regular and irregular patterns in semiarid vegetation. *Science* **284**, 1826–1828 (1999).
16. M. Pascual, F. Guichard, Criticality and disturbance in spatial ecological systems. *Trends Ecol. Evol.* **20**, 88–95 (2005).
17. S. Kéfi *et al.*, Early warning signals of ecological transitions: Methods for spatial patterns. *PLoS ONE* **9**, e92097 (2014).
18. J. Vandermeer, I. Perfecto, S. M. Philpott, Clusters of ant colonies and robust criticality in a tropical agroecosystem. *Nature* **451**, 457–459 (2008).
19. L. A. Segel, J. L. Jackson, Dissipative structure: An explanation and an ecological example. *J. Theor. Biol.* **37**, 545–559 (1972).
20. L. A. Segel, S. A. Levin, Application of nonlinear stability theory to the study of the effects of diffusion on predator–prey interactions. *AIP Conf. Proc.* **27**, 123–152 (1976).
21. S. M. Philpott, I. Perfecto, J. Vandermeer, S. Uno, Spatial scale and density dependence in a host parasitoid system: An arboreal ant, *Azteca instabilis*, and its *Pseudacteon phorid* parasitoid. *Environ. Entomol.* **38**, 790–796 (2009).
22. D. Jackson, J. Vandermeer, I. Perfecto, S. M. Philpott, Population responses to environmental change in a tropical ant: The interaction of spatial and temporal dynamics. *PLoS ONE* **9**, e97809 (2014).
23. S. Kéfi *et al.*, Spatial vegetation patterns and imminent desertification in Mediterranean arid ecosystems. *Nature* **449**, 213–217 (2007).
24. Q. X. Liu *et al.*, Pattern formation at multiple spatial scales drives the resilience of mussel bed ecosystems. *Nat. Commun.* **5**, 5234 (2014).
25. J. V. D. Koppel, M. Rietkerk, N. Dankers, P. M. Herman, Scale-dependent feedback and regular spatial patterns in young mussel beds. *Am. Nat.* **165**, E66–E75 (2005).
26. J. Vandermeer, S. Yitbarek, Self-organized spatial pattern determines biodiversity in spatial competition. *J. Theor. Biol.* **300**, 48–56 (2012).
27. J. Vandermeer, I. Perfecto, Endogenous spatial pattern formation from two intersecting ecological mechanisms: the dynamic coexistence of two noxious invasive ant species in Puerto Rico. *Proc. R. Soc. B* **287**, 20202214 (2020).
28. K. Siteur *et al.*, Phase-separation physics underlies new theory for the resilience of patchy ecosystems. *Proc. Natl. Acad. Sci. U.S.A.* **120**, e2202683120 (2023).
29. S. Kéfi *et al.*, Robust scaling in ecosystems and the meltdown of patch size distributions before extinction. *Ecol. Lett.* **14**, 29–35 (2011).
30. G. S. Bradburd, P. L. Ralph, Spatial population genetics: It’s about time. *Annu. Rev. Ecol. Evol. Syst.* **50**, 427–449 (2019).
31. A. J. Shirk, S. A. Cushman, Spatially-explicit estimation of Wright’s neighborhood size in continuous populations. *Front. Ecol. Evol.* **2**, 62 (2014).
32. Z. B. Hancock, R. H. Toczydlowski, G. S. Bradburd, A spatial approach to jointly estimate Wright’s neighborhood size and long-term effective population size. *Genetics* **227**, iyae094 (2024).
33. K. S. Korolev, J. B. Xavier, D. R. Nelson, K. R. Foster, A quantitative test of population genetics using spatiogenetic patterns in bacterial colonies. *Am. Nat.* **178**, 538–552 (2011).

34. J. A. Castillo Vardaro *et al.*, Resource availability and heterogeneity shape the self-organisation of regular spatial patterning. *Ecol. Lett.* **24**, 1880–1891 (2021).
35. M. Rietkerk *et al.*, Self-organization of vegetation in arid ecosystems. *Am. Nat.* **160**, 524–535 (2002).
36. K. Li, J. H. Vandermeer, I. Perfecto, Disentangling endogenous versus exogenous pattern formation in spatial ecology: A case study of the ant *Azteca sericeasur* in southern Mexico. *R. Soc. Open Sci.* **3**, 160073 (2016).
37. J. Vandermeer, I. Perfecto, S. M. Philpott, Ecological complexity and pest control in organic coffee production: Uncovering an autonomous ecosystem service. *BioScience* **60**, 527–537 (2010).
38. J. Vandermeer, I. Perfecto, H. Liere, Evidence for hyperparasitism of coffee rust (*Hemileia vastatrix*) by the entomogenous fungus, *Lecanicillium lecanii*, through a complex ecological web. *Plant Pathol.* **58**, 636–641 (2009).
39. D. Jackson, J. Vandermeer, I. Perfecto, Spatial and temporal dynamics of a fungal pathogen promote pattern formation in a tropical agroecosystem. *Open Ecol. J.* **2**, 62–73 (2009).
40. J. Vandermeer *et al.*, The community ecology of herbivore regulation in an agroecosystem: Lessons from complex systems. *BioScience* **69**, 974–996 (2019).
41. J. A. Wiens, Spatial scaling in ecology. *Funct. Ecol.* **3**, 385–397 (1989).
42. N. B. Kotliar, J. A. Wiens, Multiple scales of patchiness and patch structure: A hierarchical framework for the study of heterogeneity. *Oikos* **59**, 253–260 (1990).
43. S. A. Levin, The problem of pattern and scale in ecology: The Robert H. MacArthur award lecture. *Ecology* **73**, 1943–1967 (1992).
44. D. S. Viana, J. M. Chase, Spatial scale modulates the inference of metacommunity assembly processes. *Ecology* **100**, e02576 (2019).
45. J. Vandermeer, D. Jackson, Stabilizing intransitive loops: Self-organized spatial structure and disjoint time frames in the coffee agroecosystem. *Ecosphere* **9**, e02489 (2018).
46. P.-C. Bürkner, brms: An R package for Bayesian multilevel models using Stan. *J. Stat. Softw.* **80**, 1–28 (2017).
47. U. Wilensky, *NetLogo*. Center for Connected Learning and Computer-Based Modeling (Northwestern University, Evanston, IL, 1999). <https://ccl.northwestern.edu/netlogo/>. Accessed 10 March 2017.
48. Z. Hajian-Forooshani, Data. Figshare. <https://doi.org/10.6084/m9.figshare.27255300.v1>. Deposited 18 October 2024.
49. Z. Hajian-Forooshani, Code. Figshare. <https://doi.org/10.6084/m9.figshare.27255234.v1>. Deposited 18 October 2024.